Supporting Information

A Co-peptoid electrocatalyst for nitrite reduction that enables selective production of ammonia

Suraj Pahar [a] and Galia Maayan*[a]

a: Schulich Faculty of Chemistry, Technion−Israel Institute of Technology, Haifa, 3200008, Israel.

*: corresponding author and email: gm92@technion.ac.il

Experimental Methods

Materials and instrumentations

Rink Amide resin was acquired from Novabiochem; 6-bromo-2,2′-bipyridine and ethanolamine were obtained from Acros organics, Israel; Bromoacetic acid and N,N′-diisopropylcarbodiimide (DIC) were sourced from Sigma Aldrich. TFA and 4'-Chloro-2,2':6',2"-terpyridine were acquired from Alfa Aesar. 2-(4'-Chloro-2,2':6',2"-terpyridine-4'-yloxy) ethylamine and 2-(2,2'-bipyridine-6-yloxy) ethylamine were synthesized following the reported method [1,2] and protection of –OH group of ethanolamine was carried out by using previously reported procedure.[3] The Reagents, solvents, HPLC grade water and acetonitrile were acquired from commercial sources and used as received without further purification, except for DMF which was dried using molecular sieves. HPLC grade solvents were used, and high purity deionized water was prepared by using nanopore Milli-Q water purification system. Aqueous phosphate buffer solutions were made by dissolving a specific portion of mono, di- and tribasic phosphate salts, and adjusting pH with added 0.1 M NaOH solution to achieve the final pH with ionic strength of 0.1 M. From this, phosphate buffers of lower buffer concentrations of 80 mM, 60 mM, 40 mM and 20 mM were made.

Peptoid oligomers were analyzed by reversed-phase HPLC and purified using preparative HPLC following the same conditions as previously reported.[4] Mass spectrometry was conducted on an Advion expression mass with electrospray ionization (ESI). UV-Vis measurements were performed using an Agilent Technologies Cary 60 UV-Vis spectrophotometer. An Agilent Cary 630 FTIR spectrometer was used to record the IR spectra (400-4000 cm^{-1}). All the conditions used for the instruments are the same as previously reported. [4]

Preparation and characterization of TBE and CoTBE

Peptoid TBE as well as all other control peptoids reported in this work were synthesized manually on Rink amide resin using the sub monomer approach at room temperature and were characterized by analytical HPLC and ESI-MS analysis according to the previously reported procedure. [4b] The **TBE** and all other control peptoids trimer were further purified by preparative-HPLC. Corresponding cobalt complexes of the peptoid TBE and all other control peptoids were prepared in methanol solution with the addition of $Co(OAc)_2$, subsequently adding $NaClO_4$.[4] Further the prepared cobalt peptoid complexes were characterized using the previously reported procedure. [4]

Electrochemical Methods

Cyclic voltammetry (CV), Linear Sweep Voltammetry (LSV) and differential pulse voltammetry (DPV) experiments were carried out on EmStat PalmSens electrochemical analyzer in a three-electrode system containing Glassy Carbon (GC) as working electrode, Ag/AgCl as reference electrode and Pt wire as counter electrode. Before each measurement, the working electrode was polished with 0.05 μm alumina paste followed by rinsing with water and finally drying in air. CVs were collected at 100 mV/s except for other specifications. DPV was obtained with the following parameters: Amplitude = 200 mV, E-step = 10 mV, pulse width = 0.01 s.

Controlled Potential Electrolysis (CPE) experiments were performed using a two-compartment cell (H-cell) closed with septum. Large surface porous carbon (spongy shape) as working electrode together with a Ag/AgCl (NaCl sat.) as reference electrode was placed in one of the compartments that was filled with a 0.5mM buffer solution of the catalyst (pH 7, phosphate buffer 0.1 M of ionic strength with 100 mM $NaNO_2$). In the other compartment, containing only the buffer solution, a mesh platinum counter electrode was used. The use of an H-cell, where the working electrode and Ag/AgCl reference electrode are separated from the Pt counter electrode by a frit, effectively prevents deposition of Pt or Ag on the working electrode, which is expected to be negligible under our experimental conditions. Before starting the experiment, nitrogen gas was purged for 10 min to remove the oxygen from the system. After CPE, the solution was tested for quantification of ammonia and hydroxylamine formation using a standard colorimetric method:[5]

1. Ammonia in the electrolyte was quantified by the indophenol method. After the CPE experiment, the CPE solution was then neutralized by adding 0.5 M H_2SO_4, then 500 μl of phenol nitroprusside solution (P6994, Sigma-Aldrich) and 500 μl of alkaline hypochlorite solution (A1727, Sigma-Aldrich) was then added to the neutralized sample. The solution was incubated for 30 min at room temperature in the dark, and the sample absorbance was analysed by UV-vis spectroscopy. A standard calibration curve was constructed by plotting Absorbance (635 nm) vs. [NH_4^+] using a known concentration of NH_4Cl.[6]
2. NH_2OH was determined by the following procedures : In the CPE solution, 1 mL of 0.05 M phosphate buffer solution, 0.8 mL of DI water, 0.2 mL of trichloroacetic acid (12 Wt %), 1 mL of 8-quinolinol(0.1 g dissolved in 10.0 mL EtOH), and 1 mL of 1 M Na_2CO_3 solution were mixed and placed in a boiling water bath for 1 min for color development. The solution was then removed from the water bath and cooled at room temperature for 20 min. The absorbance was measured at 705 nm on a UV-vis spectrophotometer. A standard calibration curve was constructed by plotting Absorbance (705 nm) vs. [NH_2OH] using a known concentration of NH_2OH.[7]

After the amount of ammonia and hydroxylamine formation were determined, turnover number (TON) and Faradaic efficiency values were calculated using the following equations:

$$FE\ (\%) = (n_e\ F\ N_{product} / Q_{net}) \times 100\%$$

where n_e is the number of electrons required to form one molecule of product (6 for ammonia and 4 for hydroxylamine), F is the Faraday constant, $N_{product}$ is the number of moles of product formed during electrolysis, and Q_{net} is the net charge passed during electrolysis ($Q_{net} = Q_{cat} - Q_{blank}$).

The turnover number (TON) was calculated as:

$TON = N_{\_product} / N_{\_cat}$

where $N_{\_cat}$ is the total number of moles of catalyst present in the working electrode compartment.

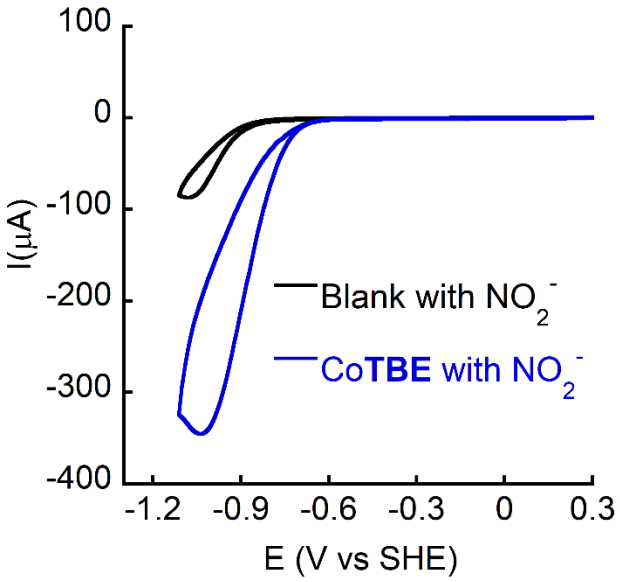

Figure S1: CVs of 100 mM $NaNO_2$ both in presence and absence of 0.5 mM Co**TBE** in 0.1 M PBS at pH 7.0.

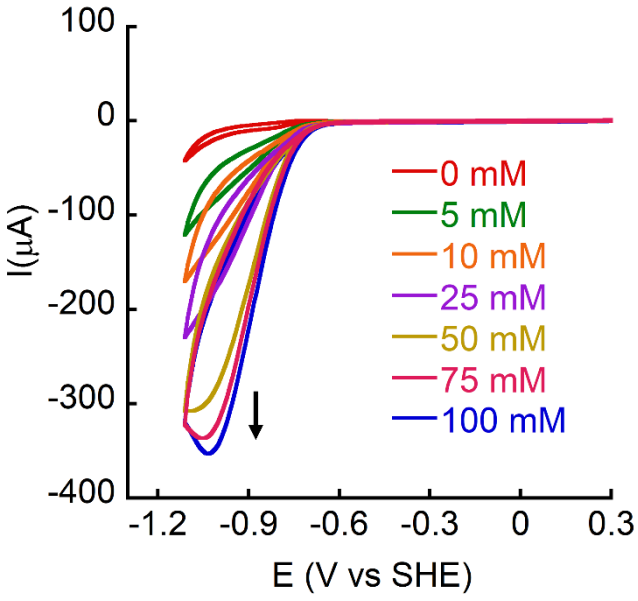

Figure S2: CVs of 0.5 mM Co**TBE** and with variable $NaNO_2$ concentration (0 to 100 mM) in 0.1 M PBS at pH 7.0.

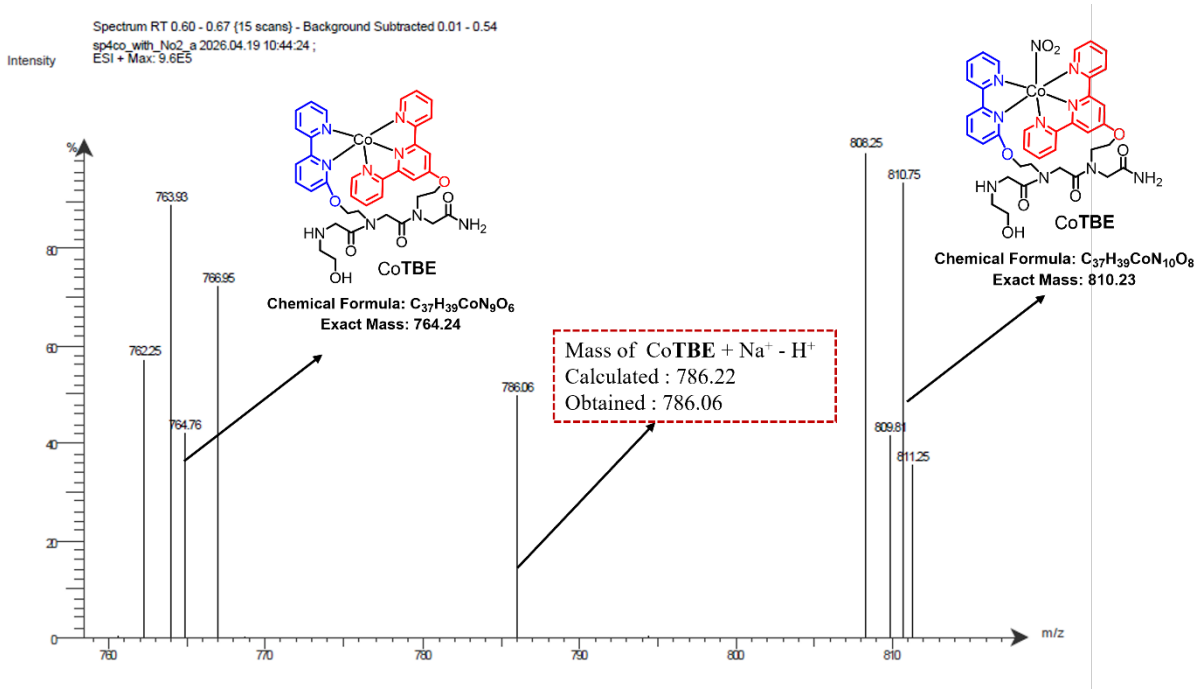

Figure S3: ESI-MS spectra of Co**TBE** in presence of $NaNO_2$.

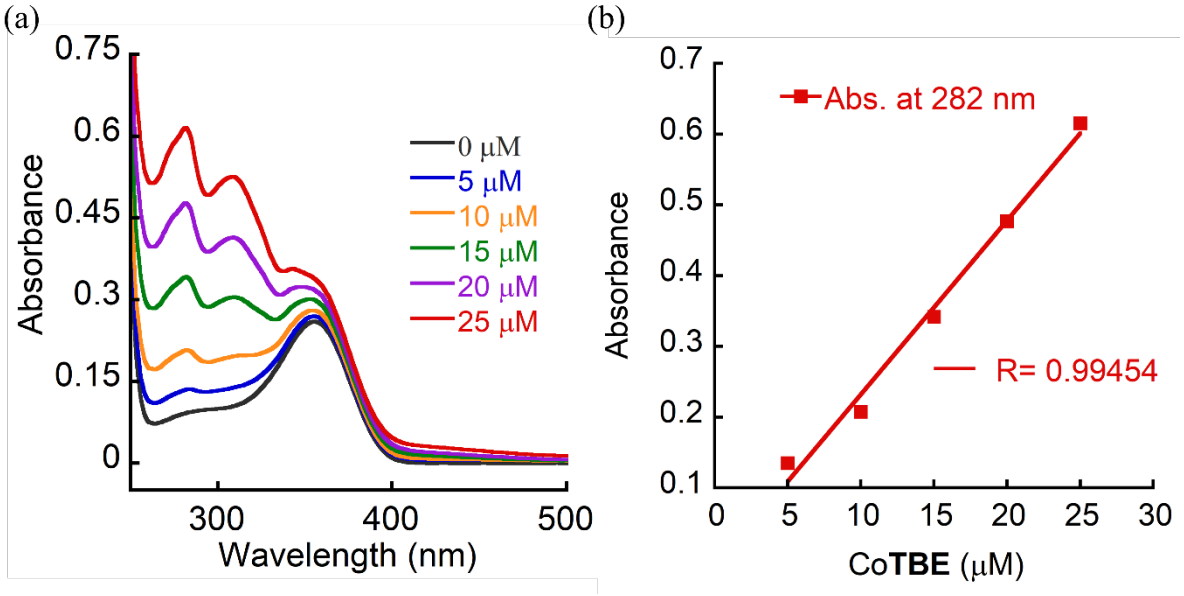

Figure S4: (a) UV–Vis spectra of Co**TBE** complex at varying concentrations in the presence of $NaNO_2$ in 0.1 M phosphate buffer at pH 7, (b) plot of linear correlation between absorbance vs. Co**TBE** concentration at λ = 282 nm.

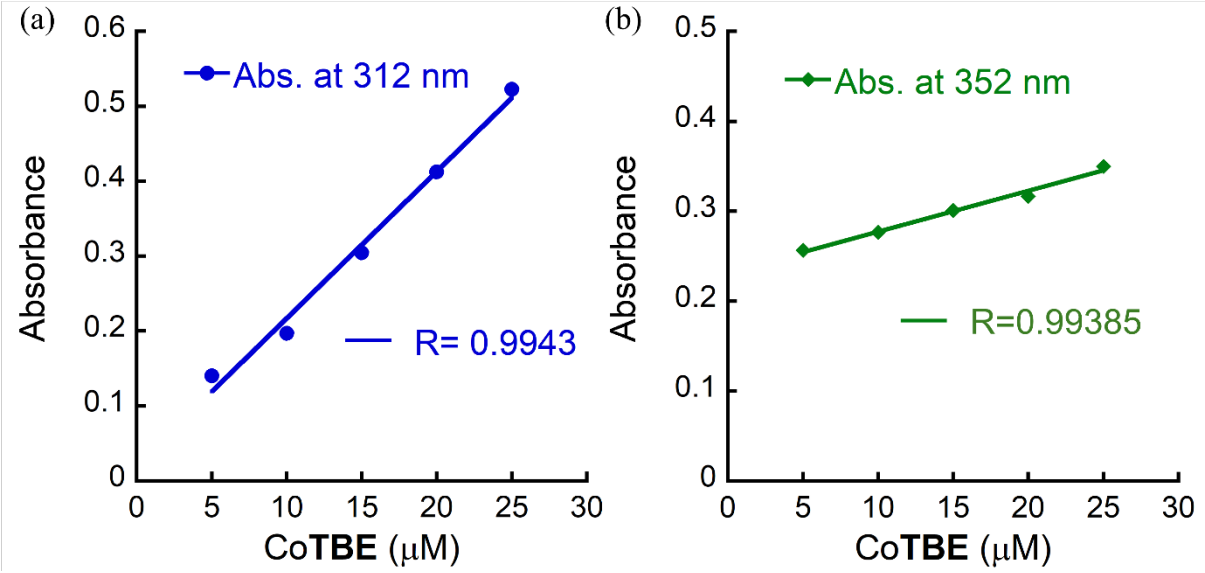

Figure S5: Plot of linear correlation between absorbance vs. Co**TBE** concentration, (a) at λ = 312 nm and (b) at λ = 352 nm.

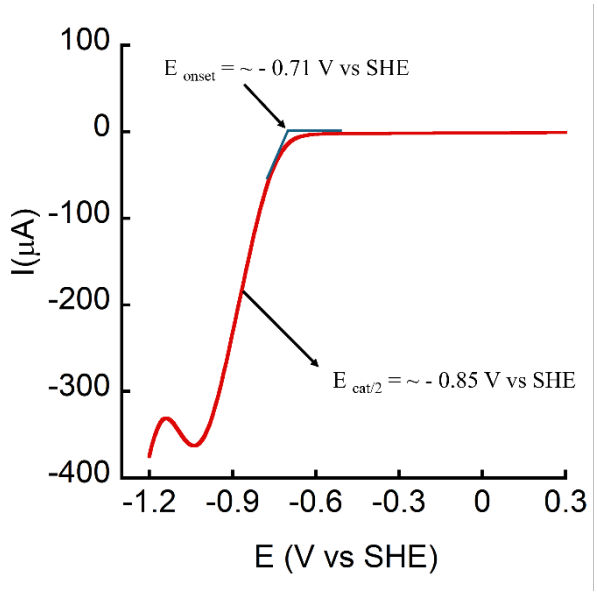

Figure S6. LSV of 0.5 mM Co**TBE** in phosphate buffer solution at pH 7 containing 100 mM $NaNO_2$.

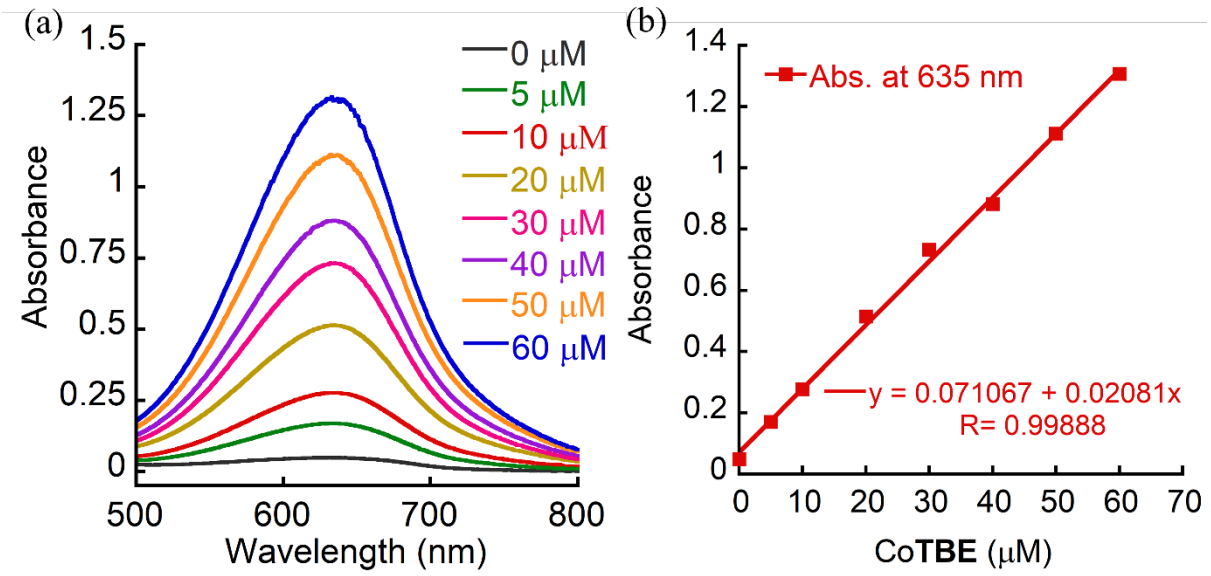

Figure S7. (a) UV-vis absorption spectra of different concentrations of NH_4Cl quantify following indophenol method, (b) resulting calibration curve.

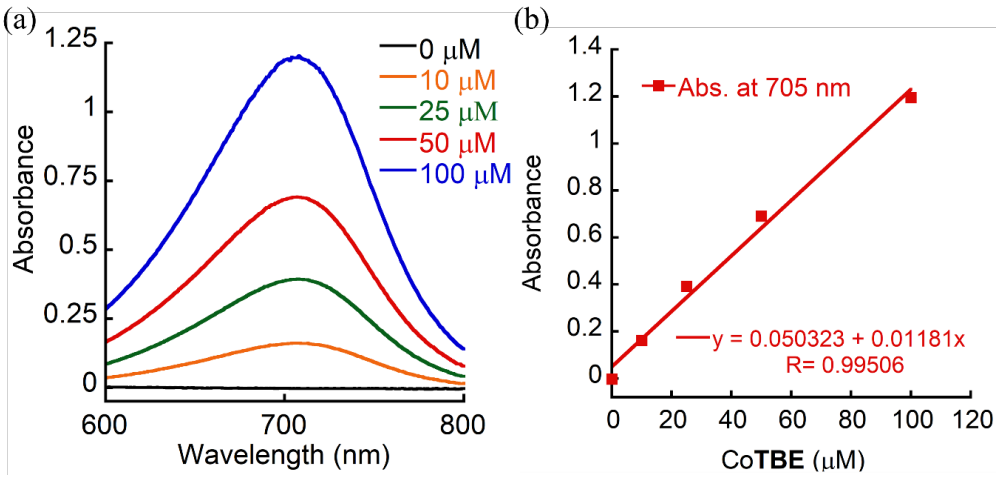

Figure S8. (a) UV-vis absorption spectra of different concentrations of NH_2OH quantify following spectrophotometric method, (b) resulting calibration curve.

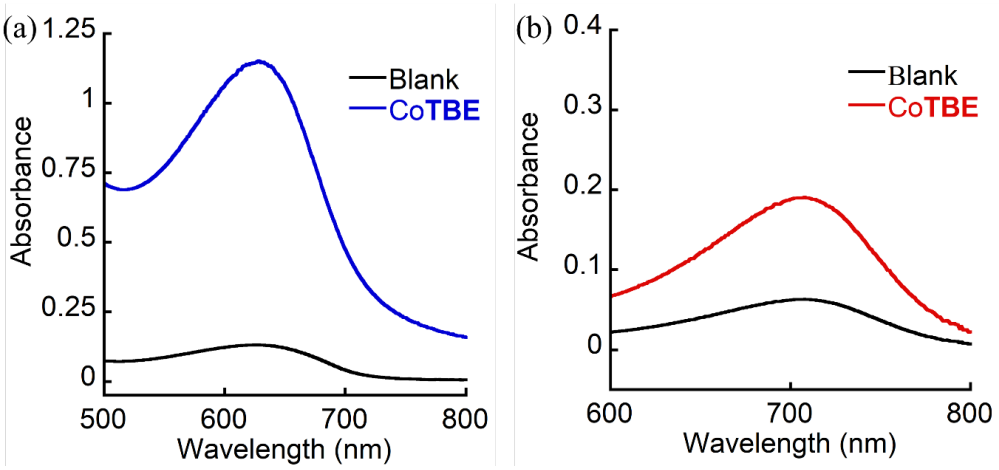

Figure S9. UV-vis absorption spectra for quantification of (a) NH_4^+ and (b) NH_2OH using spectrophotometric method of the solution after 2 hours of CPE at -1.05 V vs Ag/AgCl containing 100 mM $NaNO_2$ with Co**TBE** and without in 0.1 M phosphate buffer at pH 7.

[CoTBE] (moles)	[NH_4^+] (moles)	[NH_2OH] (moles)	Q_{blank}(C)	Q_{cat}(C)	Q_{net}(C)
2.50×10^{-6}	3.66×10^{-5}	8.18×10^{-6}	10.36	37.65	27.29
TON (NH_4^+)	**TON (NH_2OH)**	**TON (Total)**	**FE% (NH_4^+)**	**FE% (NH_2OH)**	**FE% (Total)**
14.6	3.27	17.9	77.7	11.6	89.3

Table S1: Details of charge passed during CPE with and without Co**TBE** (0.5 mM) in 0.1 M PBS (100 mM $NaNO_2$, pH 7.0, 2 h). Faradaic efficiency (FE%) were determined from the net charge passed and standard colorimetrically quantified NH_4^+ and NH_2OH.

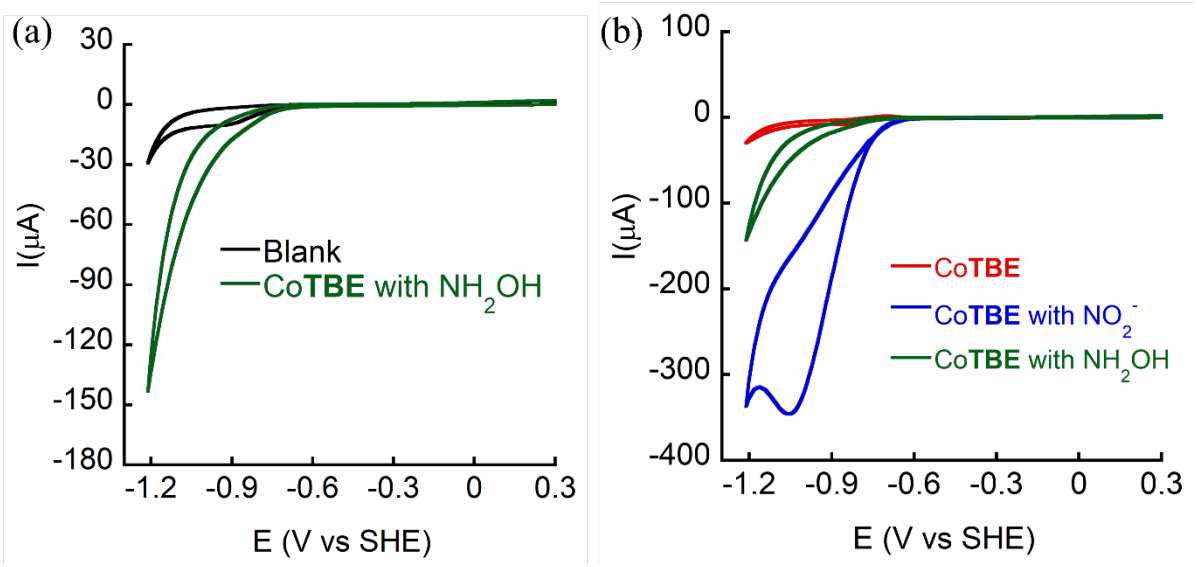

Figure S10. (a) CVs of 100 mM NH_2OH both in presence and absence of 0.5 mM Co**TBE** (b) CV of 0.5 mM Co**TBE** (red line) in the presence of 100 mM nitrite (blue) or NH_2OH (green). CVs were performed in in 0.1 M PBS at pH 7.0.

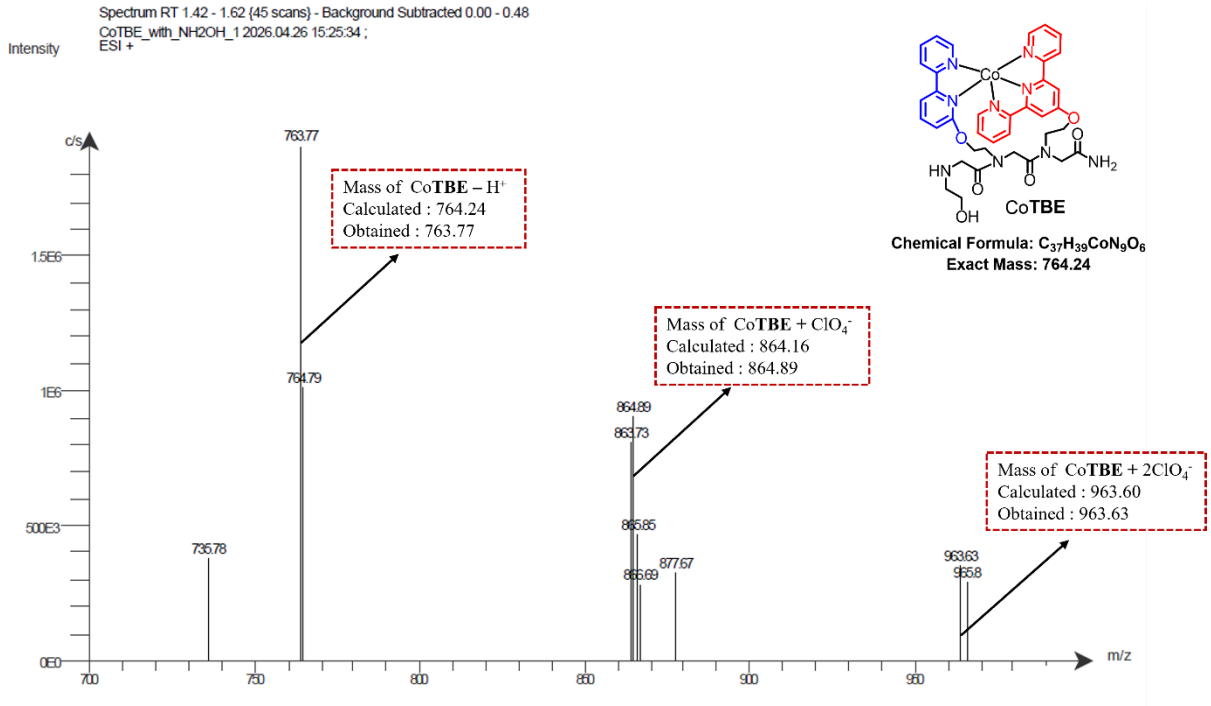

Figure S11: ESI-MS spectra of Co**TBE** in presence of NH_2OH.

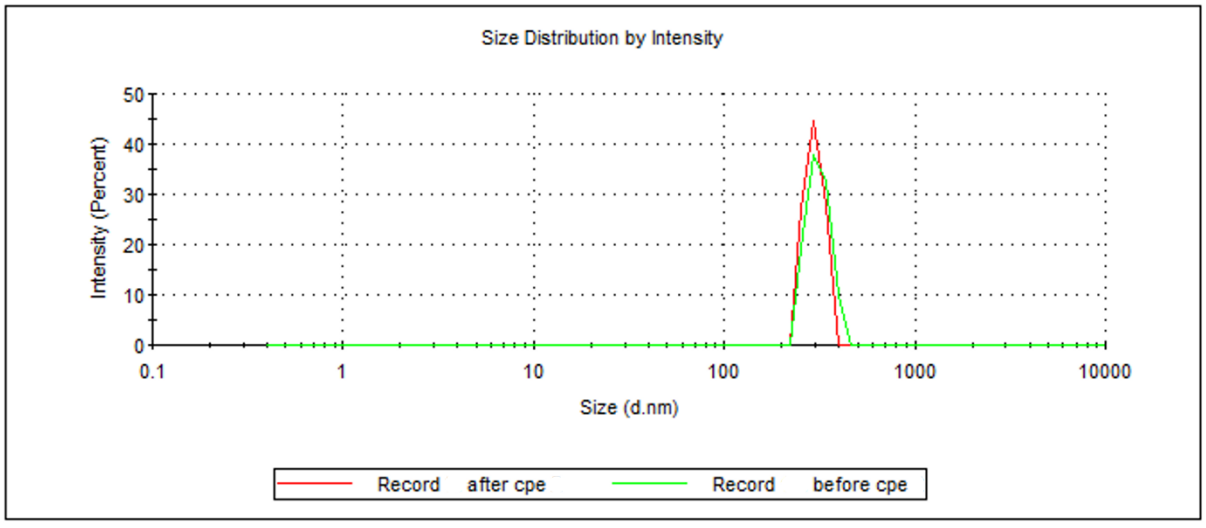

Figure S12. DLS spectra of Co**TBE** solution containing 100 mM $NaNO_2$ in 0.1 M phosphate buffer at pH 7 before (green spectra) and after (red spectra) CPE experiment.

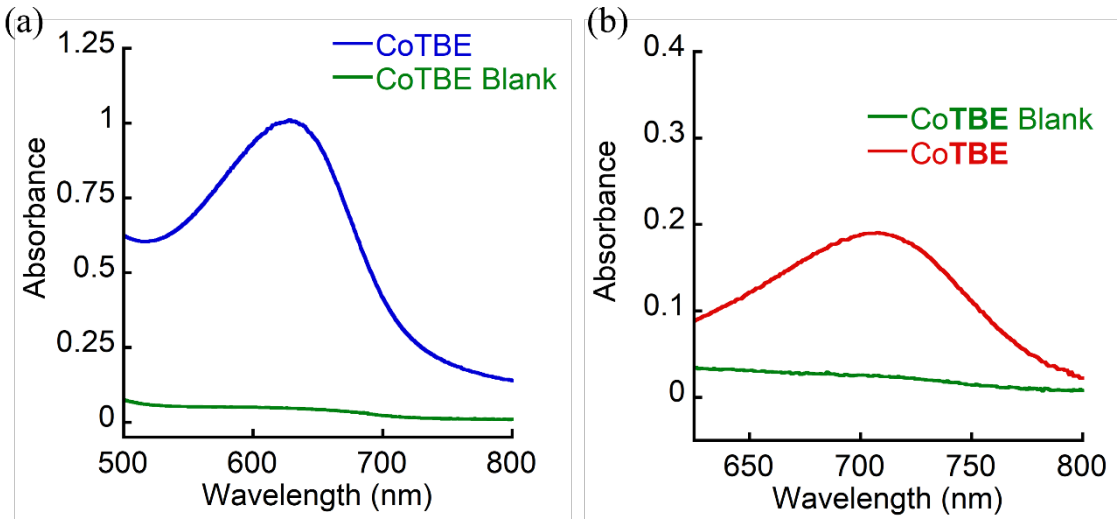

Figure S13. The detection of NH_4^+ and NH_2OH in a reaction solution containing 0.5 mM Co**TBE** and 100 mM $NaNO_2$ in PBS (pH 7.0) after stirring at room temperature for 2 h in the presence (Co**TBE**) and absence (Co**TBE** blank) of an applied potential.

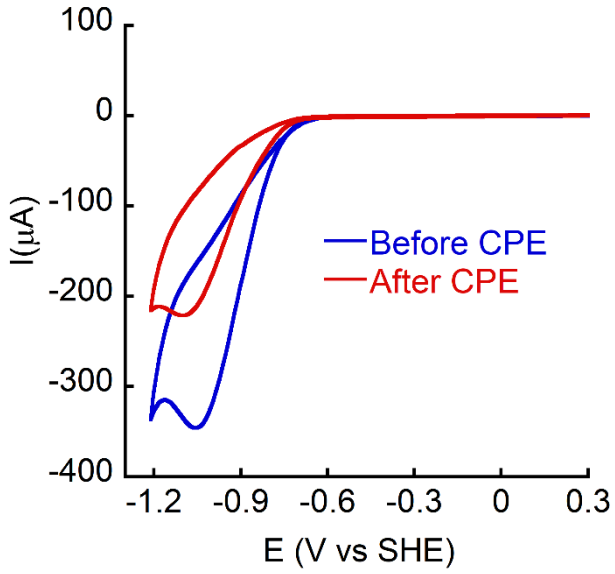

Figure S14: CV of 0.5 mM Co**TBE** containing 100 mM $NaNO_2$ before and after the CPE experiment at a potential of -0.85 V vs SHE for 2 hours in 0.1 M PBS at pH 7.0.

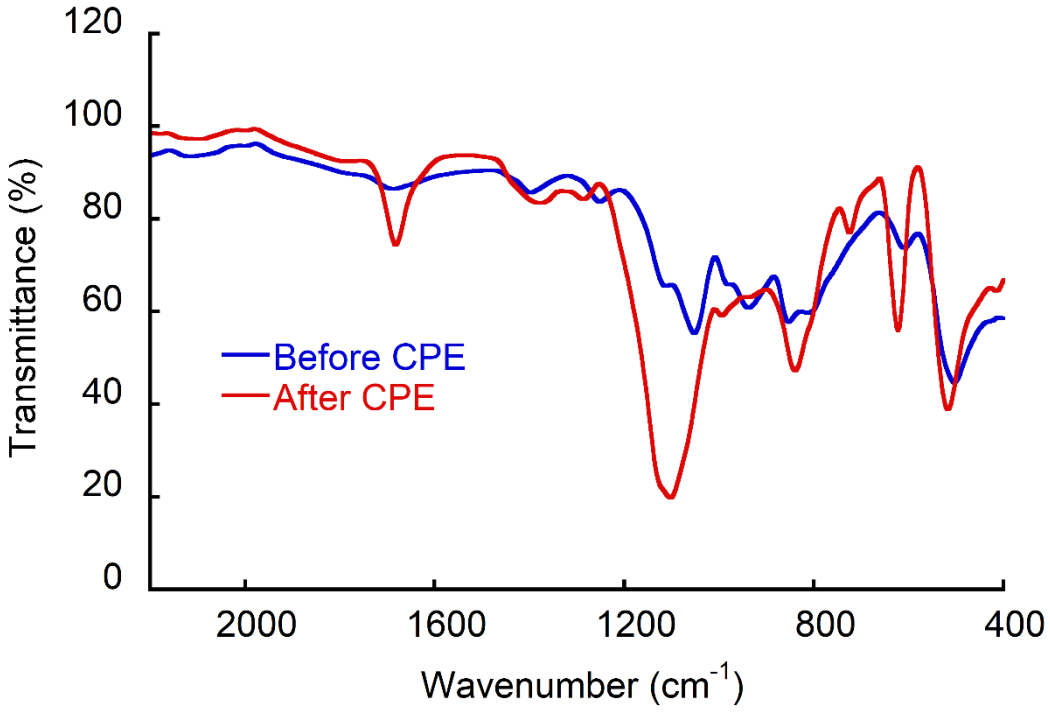

Figure S15. FTIR of the dried solid complex Co**TBE** before and after a 2-hour CPE experiment with -0.85 V vs SHE applied potential in 0.1 M phosphate buffer at pH 7 containing 100 mM $NaNO_2$.

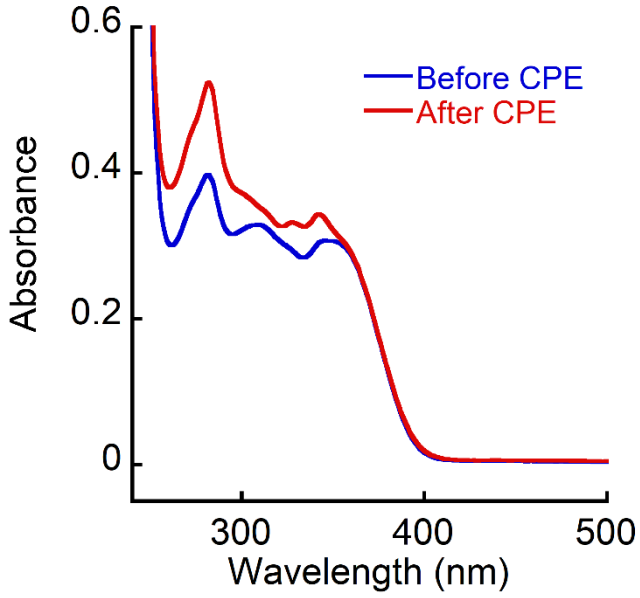

Figure S16. UV-Vis absorption spectra of Co**TBE** before and after a 2-hour CPE experiment with -0.85 V vs SHE applied potential in 0.1 M phosphate buffer at pH 7 containing 100 mM $NaNO_2$.

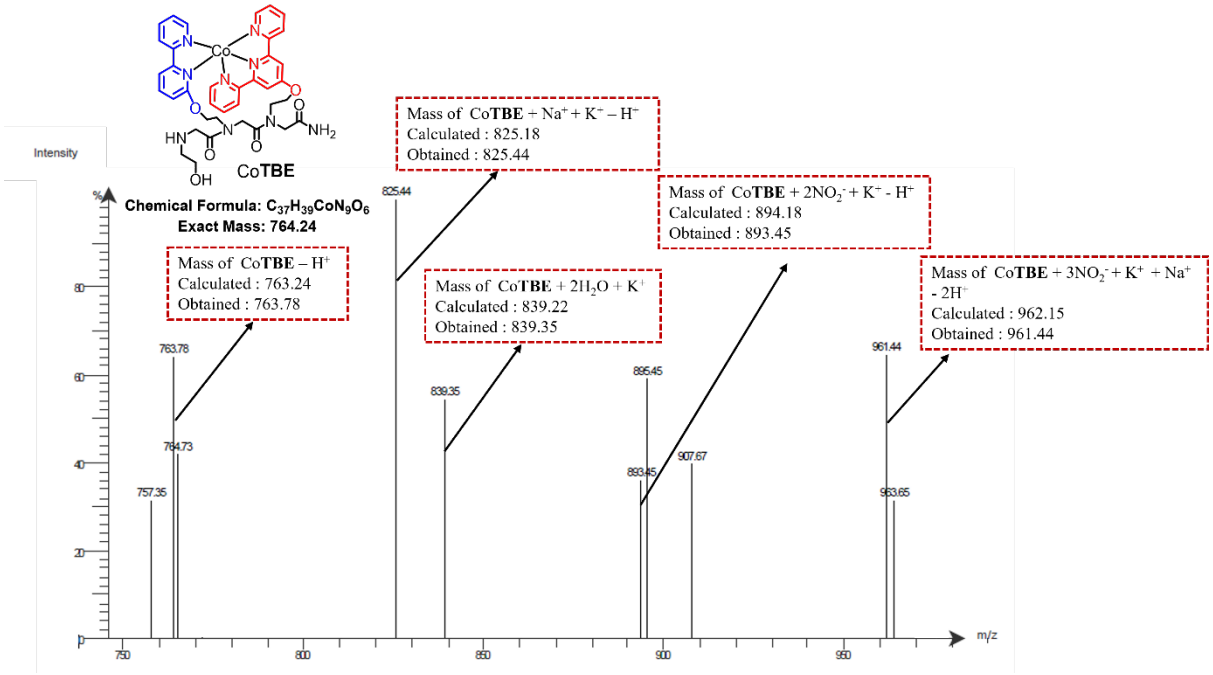

Figure S17. ESI-MS of the catalytic solution of Co**TBE** before CPE in 0.1M phosphate buffer solution at pH = 7.0 containing 100 mM $NaNO_2$.

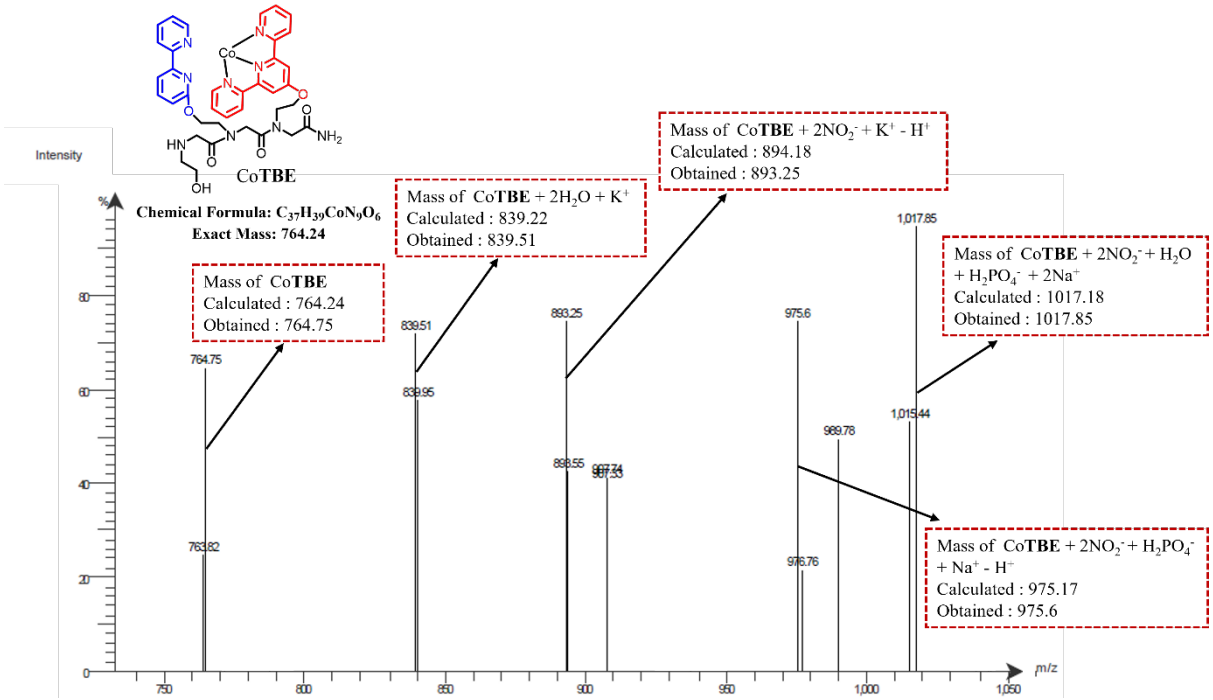

Figure S18. ESI-MS of the catalytic solution of Co**TBE** after CPE in 0.1M phosphate buffer solution at pH = 7.0 containing 100 mM $NaNO_2$.

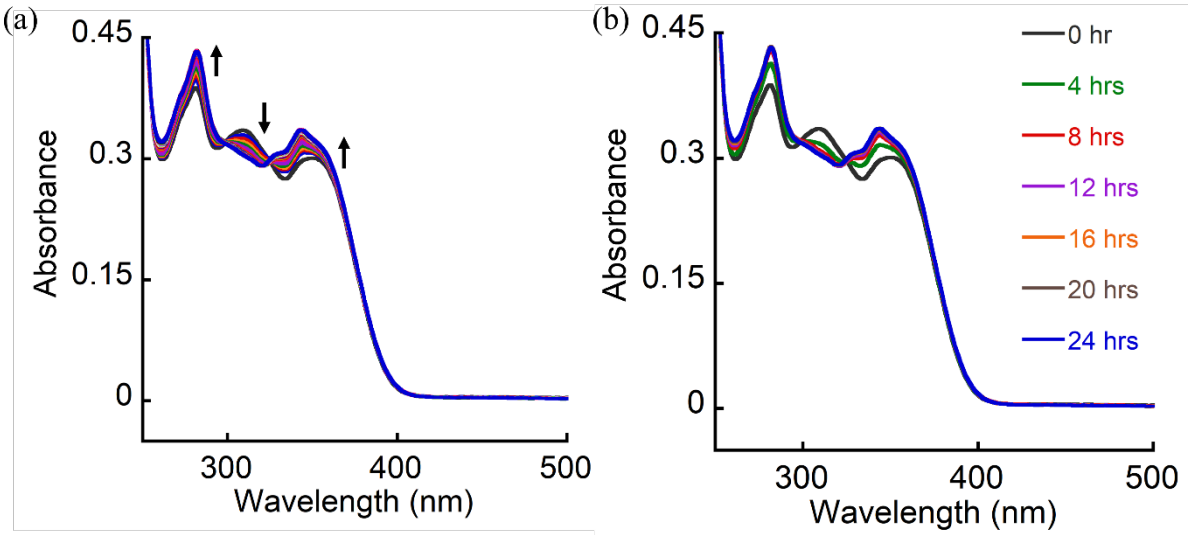

Figure S19. UV-Vis absorption spectra of~20 µM of Co**TBE** with $NaNO_2$ in 0.1M phosphate buffer at pH 7 without disturbing for 24 hours, (a) Complete set of spectra over the entire duration, (b) Spectra extracted at 4 h intervals.

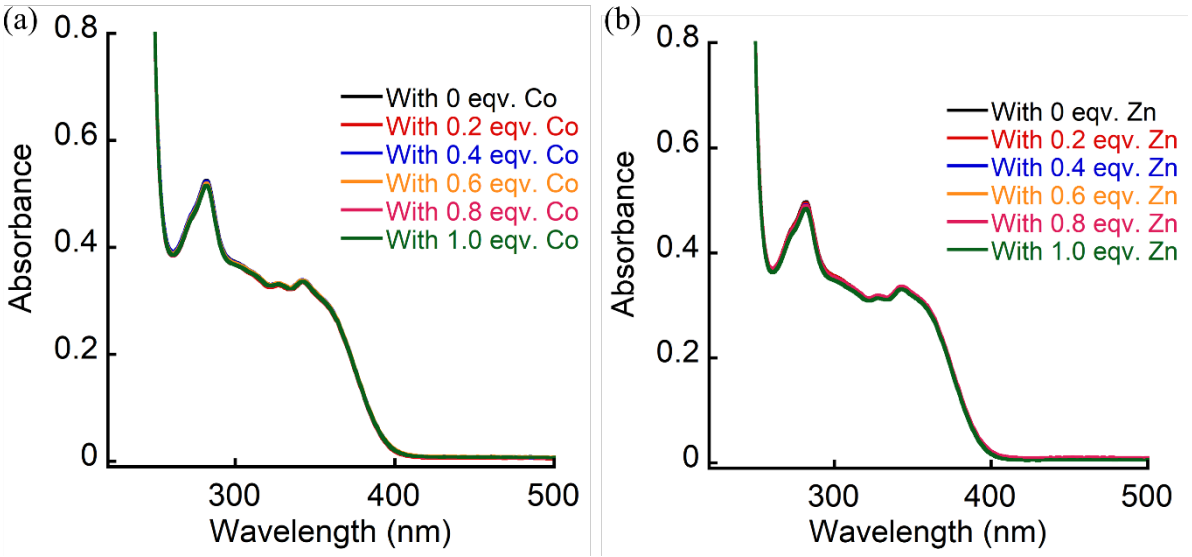

Figure S20. UV-Vis titration spectra of~20 µM of Co**TBE** with $NaNO_2$ in 0.1M phosphate buffer at pH 7 after 24 hours of undisturbed incubation: (a) Co and (b) Zn.

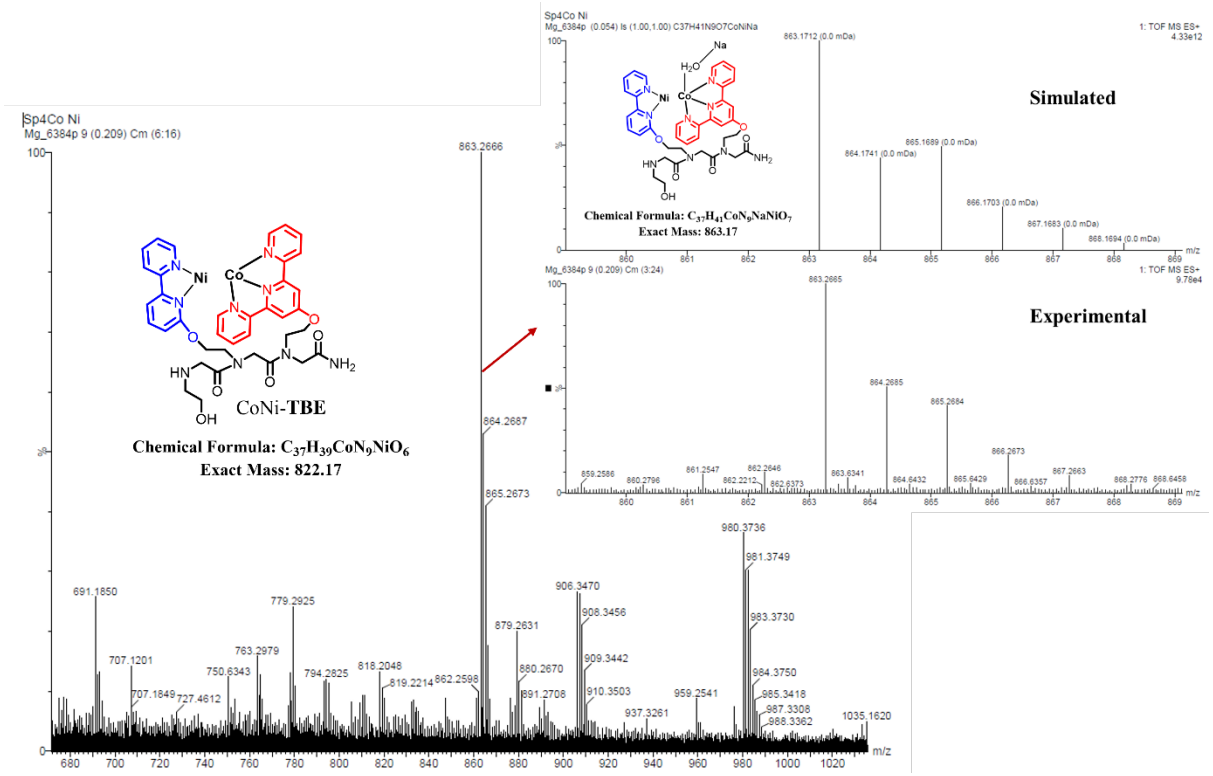

Figure S21. HR-MS of the isolated solution of UV-Vis titration of Co**TBE** with Ni in 0.1M phosphate buffer at pH 7 containing $NaNO_2$ after 24 hours of undisturbed incubation.

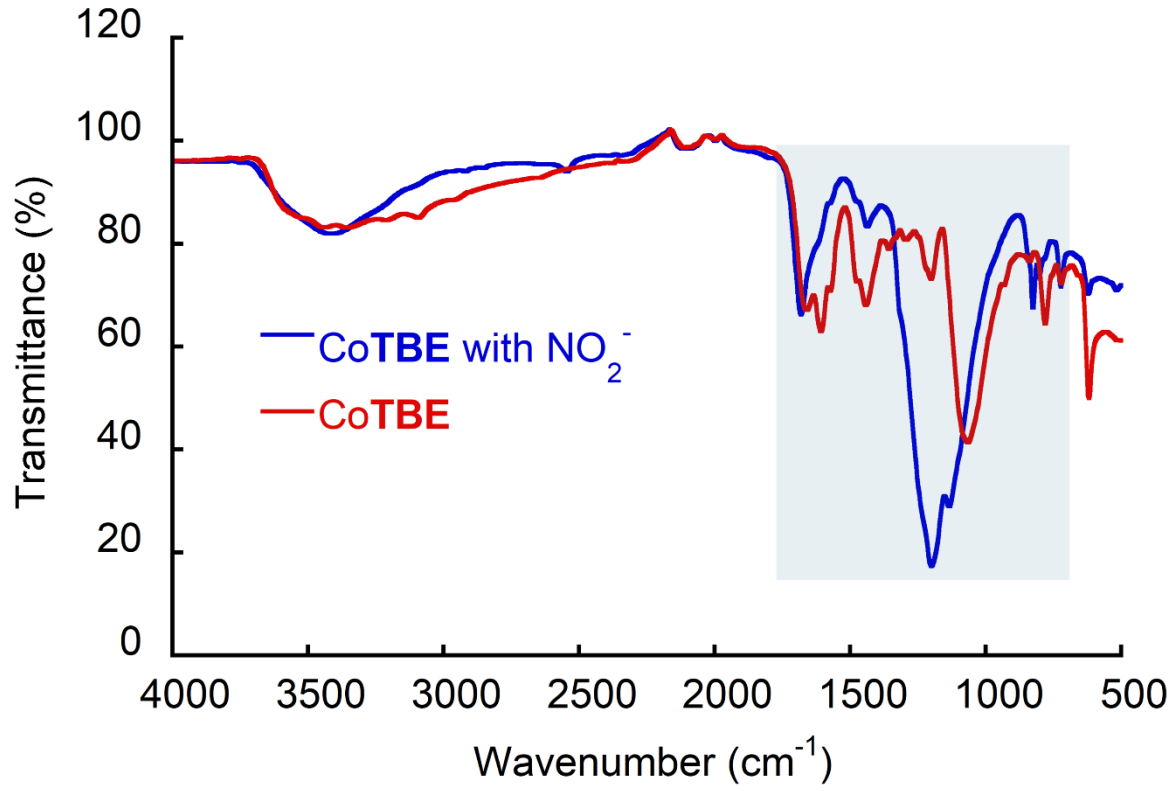

Figure S22. FTIR spectra of Co**TBE** and the dried solid complex of Co**TBE** solution with $NaNO_2$.

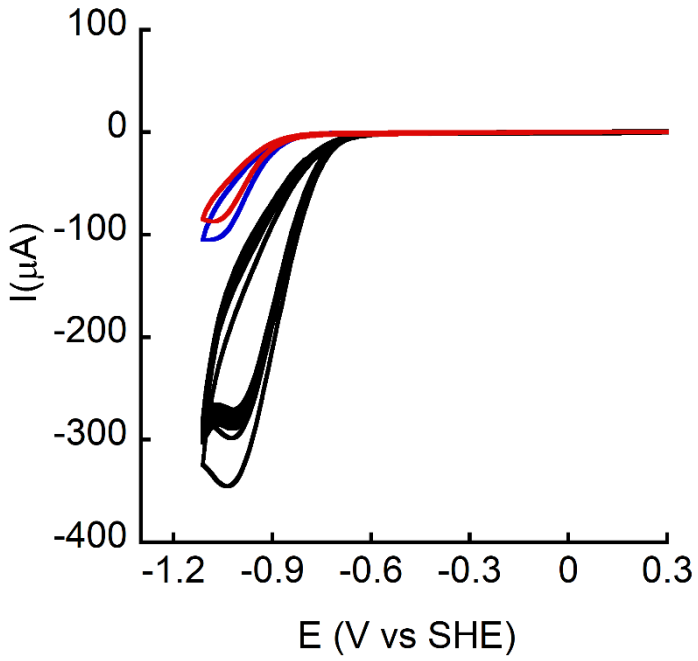

Figure S23. Continuous 20 CVs of 0.5 mM Co**TBE** (black) with 100 mM $NaNO_2$, buffer solution containing 100 mM $NaNO_2$ without catalyst (red), and blank buffer solution containing 100 mM $NaNO_2$ recorded after rinse the electrode with water without polishing (blue). All CVs were measured in 0.1 M phosphate buffer solution at pH 7.

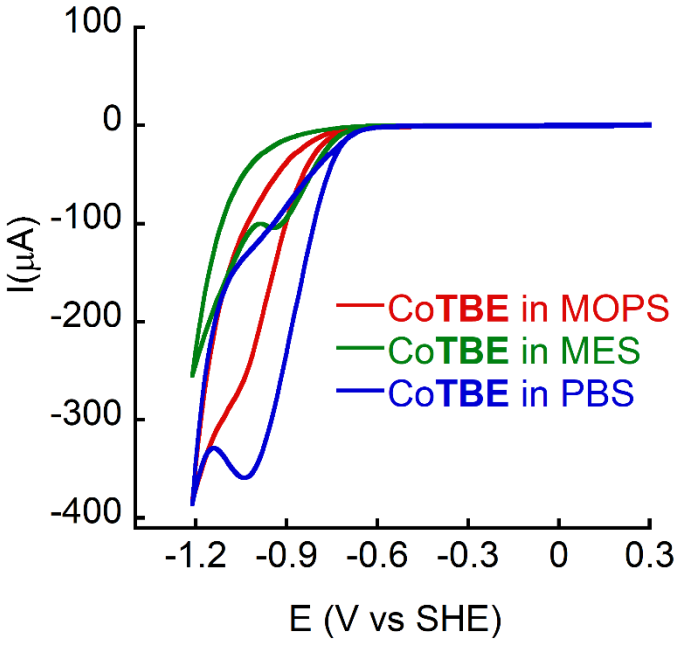

Figure S24. CVs of 0.5 mM Co**TBE** in different buffers at pH 7 with 100 mM $NaNO_2$.

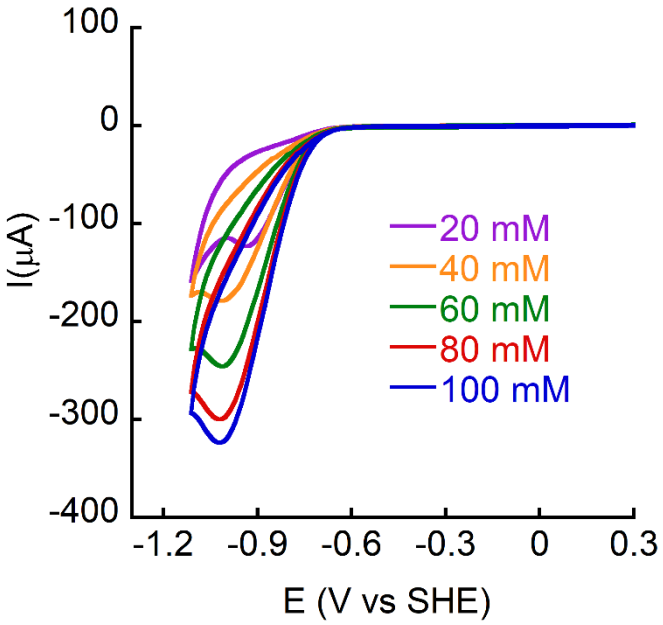

Figure S25. CVs of 0.5 mM Co**TBE** in varying concentration of phosphate buffer at pH 7 with 100 mM $NaNO_2$.

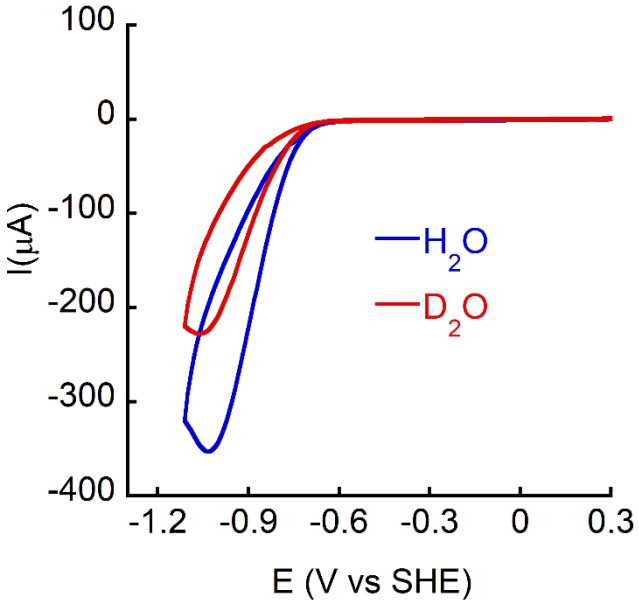

Figure S26. CVs of 0.5 mM Co**TBE** in H_2O and D_2O in 0.1M phosphate buffer at pH 7 with 100 mM $NaNO_2$.

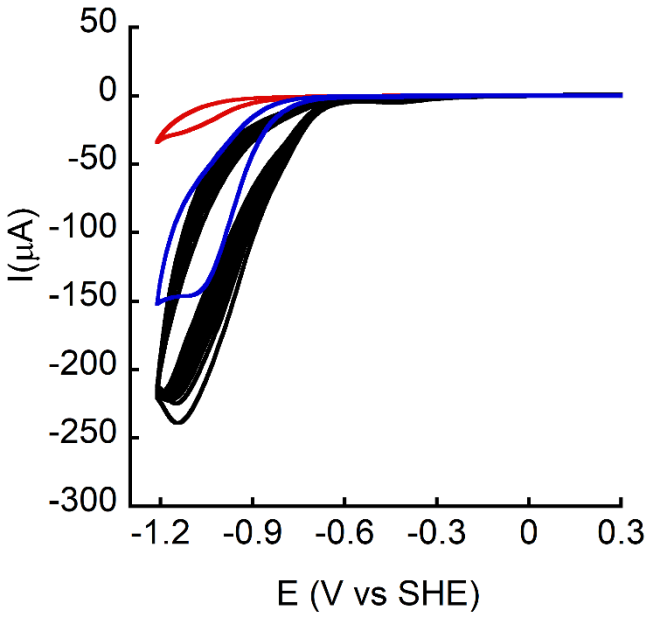

Figure S27. Continuous CV scans of 0.5 mM Co**TB-BZ** (black) with 100 mM $NaNO_2$, buffer solution containing 100 mM $NaNO_2$ without catalyst (red), and blank buffer solution containing 100 mM $NaNO_2$ recorded after rinse the electrode with water without polishing (blue). All CVs were measured in 0.1 M phosphate buffer solution at pH 7.

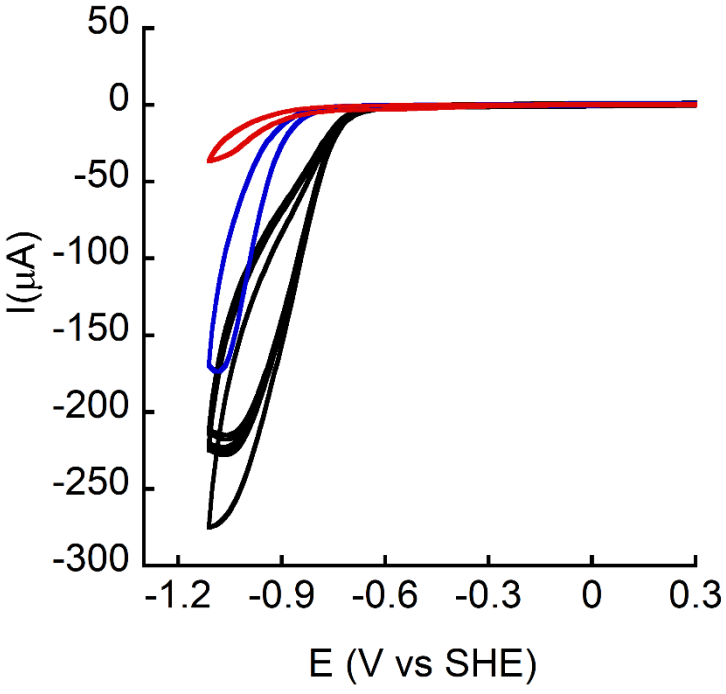

Figure S28. Continuous CV scans of 0.5 mM Co**TB** (black) with 100 mM $NaNO_2$, buffer solution containing 100 mM $NaNO_2$ without catalyst (red), and blank buffer solution containing 100 mM $NaNO_2$ recorded after rinse the electrode with water without polishing (blue). All CVs were measured in 0.1 M phosphate buffer solution at pH 7.

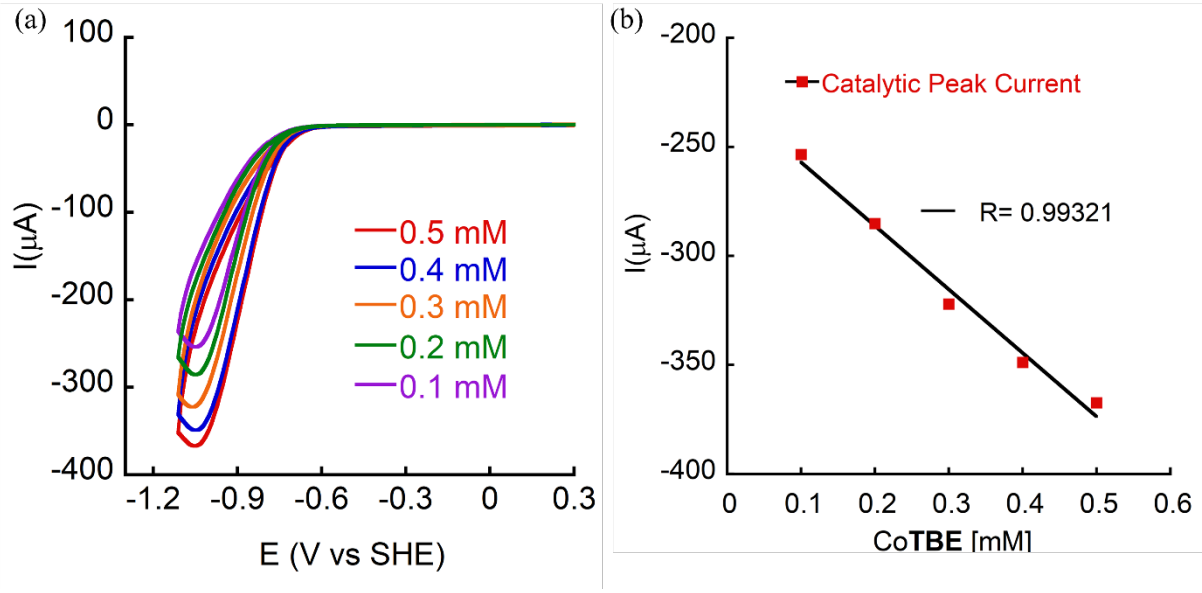

Figure S29: (a) CVs of Co**TBE** having different concentration in 0.1 M PBS at pH 7 with 100 mM $NaNO_2$ (b) Linear regression of catalytic peak current versus different concentration of Co**TBE**.

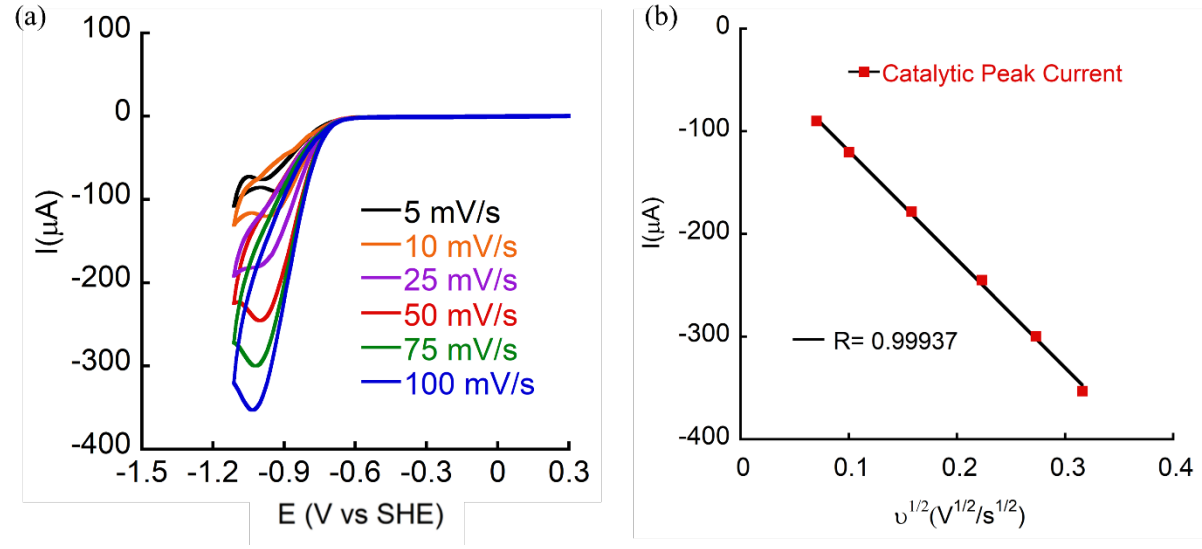

Figure S30: (a) CVs of 0.5 mM Co**TBE** at different scan rates in 0.1 M phosphate buffer pH 7 with 100 mM NO_2^- (b) Linear regression of catalytic peak current versus root of scan rates.

Table S2. Data summary of Co-based electrocatalysts for homogeneous nitrite reduction from reported literature:

Catalyst	Product(s)	Applied Potential (V) (reference)	FE% Yield & TON	Experimental Conditions	Reference
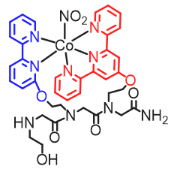	NH_4^+ and NH_2OH	-0.85 (SHE)	NH_4^+, 78%, NH_2OH, 12% 18	pH = 7, 0.1 M phosphate buffer	Present work
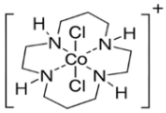	NH_4^+ and NH_2OH	-1.5 (SCE)	NH_4^+, 6% NH_2OH, 73% ----	Hg electrode, 3M NaOH,	8
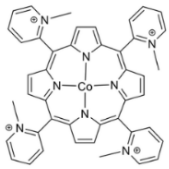	NH_4^+ and NH_2OH	-0.7 (Ag/AgCl)	NH_4^+, 33% NH_2OH, 60% ----	pH = 5 buffer, carbon rod electrode	9
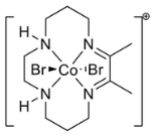	NH_4^+	-1.05 (SCE)	88% 18.9	pH = 7.2, aqueous solution	10
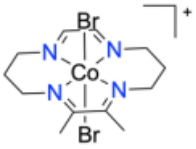	NH_4^+ and NH_2OH	-0.9 (SCE)	NH_4^+, 17% NH_2OH, 85% ----	pH= 7, 0.5 M phosphate buffer solution	11
	NH_4^+ and NH_2OH	-1.25 (SCE)	NH_4^+, 30% NH_2OH, 47% ----	0.75 M MOPS buffer	12
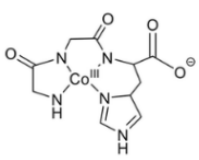	NH_4^+	−0.90 (Ag/AgCl)	90% 3550	1M MOPS buffer, pH = 7.2, Hg electrode	13

References:

1. G. Maayan, B. Yoo, K. Kirshenbaum, Tetrahedron Lett 50 (2009) 4297-4297.
2. M. Baskin, L. Panz, G. Maayan, Chem. Commun., 2016, 52, 10350-10353
3. T.W. Green and P.G.M. Wuts, Protective Groups in Organic Synthesis, Wiley Interscience (1999) 127-141 708-711.
4. (a) G. Ruan, L. Engelberg, P. Ghosh, G. Maayan, Chem. Commun., 2021, 57, 939-942, (b) S. Pahar, G. Maayan, Chem. Sci. 2024, 15, 12928–12938.
5. (a) M. W. Weatherburn, *Anal. Chem*. 1967, 39, 971– 974. (b) D.S. Frear, and R.C. Burrell, *Anal. Chem*. 1955, 27(10), 1664-1665.
6. S. Z. Andersen, V. Colic, S. Yang, J. A. Schwalbe, A. C. Nielander, J.M. Mcenaney, K. Enemark-Rasmussen, J. G. Baker, A. R. Singh, B.A. Rohr, M. J. Statt, S. J. Blair, S. Mezzavilla, J. Kibsgaard, P. C. K.Vesborg, M. Cargnello, S. F. Bent, T. F. Jaramillo, I. E. L. Stephens, J.K. Nørskov, I. Chorkendorff, *Nature* 2019, 570, 504.
7. H. Dong, X. Wang, P. Shi, N. Chen, Z. Zhang, J. Yan, A. Lei and H Yi, *J. Am. Chem. Soc.* 2025, 147, 32, 29423–29430.
8. H.L. Li, W. C. Anderson, J. Q. Chambers, D. T. Hobbs, Inorg. Chem. 1989, 28 (5), 863–868.
9. S.-H. Cheng, Y. O. Su. Inorg. Chem. 1994, 33, 5847-5854.
10. S. Xu, H.-Y. Kwon, D. C. Ashley, C.-H. Chen, E. Jakubikova, J. M. Smith, Inorg. Chem. 2019, 58, 9443-9451.
11. S. E. Braley, H.-Y. Kwon, S. Xu, E. Z. Dalton, E. Jakubikova, J. M.Smith, Inorg. Chem. 2022, 61, 12998-13006.
12. S. Partovi, E. Z. Dalton, J. M. Smith, ACS Catal. 2024, 14, 7756-7761.
13. Y. Guo, J. R. Stroka, B. Kandemir, C. E. Dickerson and K. L. Bren, J. Am. Chem. Soc., 2018, 140, 16888–16892.